Eur. Phys. J. A **17**, 483–487 (2003)
DOI 10.1140/epja/i2002-10199-0

THE EUROPEAN PHYSICAL JOURNAL A

Electromagnetic and weak transitions in light nuclei

M. Viviani[1,a], L.E. Marcucci[2], A. Kievsky[1], S. Rosati[2], and R. Schiavilla[3,4]

[1] INFN, Sezione di Pisa, Via Buonarroti 2, I-56100 Pisa, Italia
[2] Dipartimento di Fisica, Università di Pisa , Via Buonarroti 2, I-56100 Pisa, Italia
[3] Jefferson Laboratory, Newport News, VA 23606, USA
[4] Physics Department, Old Dominion University, Norfolk, VA 23529, USA

Received: 1 November 2002 /
Published online: 15 July 2003 –

Abstract. Recent advances in the study of the p-d radiative and μ-^{3}He weak capture processes by our group are presented and discussed. The trinucleon bound and scattering states have been obtained from variational calculations by expanding the corresponding wave functions in terms of correlated hyperspherical harmonic functions. The electromagnetic and weak transition currents include one- and two-body operators. The accuracy achieved in these calculations allows for interesting comparisons with experimental data.

PACS. 21.45.+v Few-body systems – 23.40.-s Beta decay; double beta decay; electron and muon capture – 25.40.Lw Radiative capture

1 Introduction

A number of electromagnetic (EM) and weak transitions in light nuclei have interesting astrophysical implications as well as important implications for an understanding of nuclear structure and dynamics. The theoretical description of these processes requires the knowledge of the initial (bound) and final (in general, continuum) nuclear states and the use of EM and weak current operators constructed consistently with the interactions used to generate the wave functions. In particular, the trinucleon system provides a unique "laboratory" due to the capability, achieved in the last few years, of obtaining very accurate bound and continuum nuclear wave functions. The accuracy of the calculated trinucleon wave functions Ψ_{3N} has been verified by comparing results for a variety of observables obtained by a number of groups using different techniques [1]. At present, a good overall agreement exists between the theoretical and experimental N-d elastic- and inelastic-scattering observables (a notable exception, however, is the A_y analyzing power at low energies) [2, 3]. Therefore, the study of EM and weak transitions in the three-nucleon system does not suffer from uncertainties related to the computation of Ψ_{3N} and is a direct test of i) the nuclear Hamiltonian H from which the nuclear wave functions are obtained, and ii) the model used to describe the nuclear currents. Since the nuclear EM current is related to H through current conservation, it is clear that the two topics are inter-related. Other important questions which can be addressed are the role that relativistic corrections as well as Δ-isobar and additional sub-nucleonic degrees of freedom play in these processes.

The nuclear EM and weak currents considered here are as in the model developed in refs. [4,5] (see also ref. [6]) and include one- and two-body operators. They have been tested in a number of few-nucleon processes. The one-body operators are obtained directly from the non-relativistic limit of the covariant single-nucleon vector and axial currents. In the study of the muon capture, the contribution coming from the induced pseudo-scalar term of the nucleon axial current has to be included (while it gives a negligible contribution to beta-decay processes). However, the experimental value of the corresponding form factor $G_{PS}(q_\sigma^2)$ is rather uncertain. Assuming pion-pole dominance, the partially conserved axial current (PCAC) hypothesis, and the Goldberger-Treiman relation, G_{PS} is predicted to be [7–9]

$$G_{PS}^{\rm PCAC}(q_\sigma^2) = -\frac{2\,m_\mu\,m_N}{m_\pi^2+q_\sigma^2}\,G_A(q_\sigma^2)\ , \qquad (1)$$

where q_σ is the four-momentum transferred to the nuclear system, m_N, m_μ and m_π indicates the nucleon, muon and pion mass, respectively, and G_A is the axial form factor. In our calculation, we have assumed

$$G_{PS}(q_\sigma^2) = R_{PS}\,G_{PS}^{\rm PCAC}(q_\sigma^2)\ , \qquad (2)$$

where R_{PS} is a parameter which has been varied to study the sensibility of our results to this form factor and to

[a] e-mail: michele.viviani@pi.infn.it

investigate to which extent $G_{PS}^{\rm expt} = G_{PS}^{\rm PCAC}$. However, most of the calculations have been performed with the choice $R_{PS} = 1$.

The two-body EM current is separated in two terms. There is a "model-independent" part which is constructed consistently with the nucleon-nucleon interaction, in order to satisfy the current conservation relation [10]. The second part includes "model-dependent" contributions which come from the $\pi\rho\gamma$ and $\pi\omega\gamma$ processes and the Δ degrees of freedom. The latter contribution is included in the current and in the nuclear medium in an approximate way, by following the procedure described in ref. [11]. The two-body weak vector current is then obtained from the isovector part of the EM current, in accordance with the conserved–vector-current hypothesis.

Two-body terms have been taken into account in both the axial charge and current operators. The two-body axial charge operator has been obtained consistently with the two-nucleon interaction model, following the methods of ref. [12]. The two-body axial current operators are derived from a meson-exchange model, including π- and ρ-exchanges and the $\rho\pi$-transition processes, as well as Δ-isobar excitation [13,14]. The latter process gives the dominant contribution. However, its magnitude depends critically on the value adopted for the $N\Delta$ axial coupling constant g_A^*. In the quark model, g_A^* is related in a simple way to the axial coupling constant of the nucleon g_A ($g_A \approx 1.26$). However, given the uncertainties inherent in quark model predictions, a more reliable estimate for g_A^* is obtained by adjusting its value to reproduce the experimental value of the Gamow-Teller matrix element in tritium β-decay [13,15]. In this way, the model dependence of the weak axial current is significantly reduced, as shown by previous studies of proton weak captures on ^{1}H [13] and ^{3}He [15].

The ^{3}He, ^{3}H bound and the p-d continuum wave functions have been calculated by means of an expansion over the pair-correlated hyperspherical harmonic (PHH) basis functions [16,17]. Such a technique has been proved to be very accurate. Various n-d elastic-scattering observables calculated by solving the Faddeev equations [2] are in remarkable agreement with the corresponding results obtained with the PHH technique. For example, the phase shift and mixing angle parameters calculated by the two methods at the center-of-mass (c.m.) energy $E_{\rm c.m.} = 2$ MeV have been found to differ at level of 0.1%, at most [1]. It should be pointed out that with the PHH technique the inclusion of the Coulomb potential, very important in the energy range considered here, does not present any difficulty.

This paper is organized as follows. The p-d radiative capture and the muon capture on ^{3}He are discussed in sects. 2 and 3, respectively. The last section contains a summary and some concluding comments.

2 Radiative p-d capture

The applications of our formalism for c.m. energies ranging from zero to 2 MeV, namely below the deuteron breakup threshold (DBT), were already presented in refs. [19] and [20]. Recently, we have extended the PHH technique, in order to compute also p-d scattering wave functions above the DBT [21]. We can therefore compute p-d capture observables at higher energies than previously published. A preliminary study at c.m. energy $E_{\rm c.m.} = 3.33$ MeV, where high-quality data, including differential cross-sections, vector and tensor analyzing powers [22] exist, are reported below.

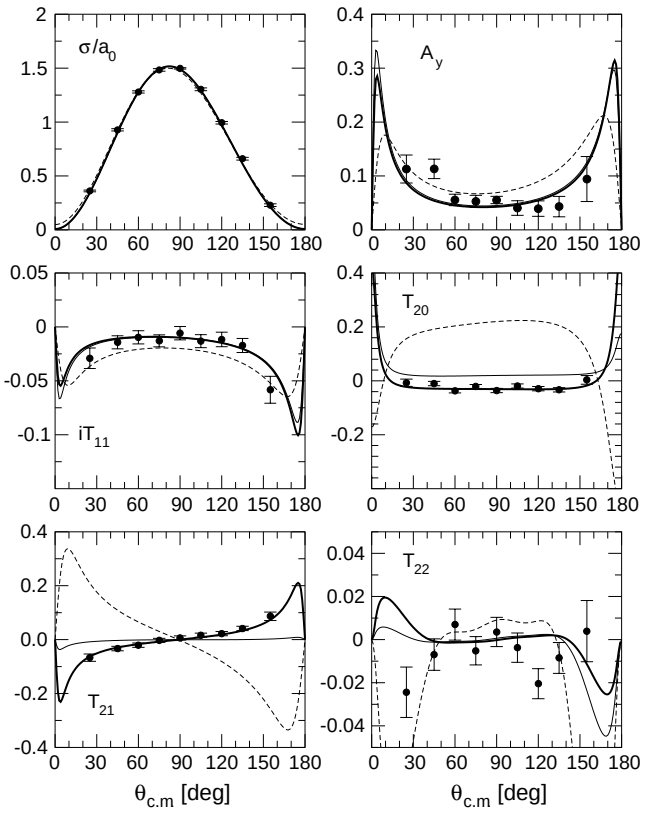

Fig. 1. Differential cross-section, proton vector analyzing power, and the four deuteron tensor analyzing powers for p-d capture at $E_{\rm c.m.} = 2$ MeV, obtained with the AV18/UIX Hamiltonian model and one-body only (dashed lines) or both one- and two-body currents (thin solid lines), are compared with the experimental values of ref. [18]. The results obtained in the long-wavelength approximation (LWA) for the spin-flip E_1 RMEs are also shown (thick solid lines). In the first panel, $a_0 = \int {\rm d}\Omega\, \sigma/(4\pi)$.

First of all, it is worth mentioning that the same set of observables were measured also at $E_{\rm c.m.} = 2$ MeV [18]. In our previous study [20], we compared the theoretical predictions with these experimental data, which, for the sake of completeness, are reported in fig. 1. All the results reported in this section have been obtained using the Argonne v_{18} (AV18) [23] two-nucleon and Urbana IX (UIX) [24] three-nucleon interactions. As can be seen by inspection of the figure, our results (thin solid lines) for the differential cross-section and the observables A_y and iT_{11} are in good agreement with the experimental data.

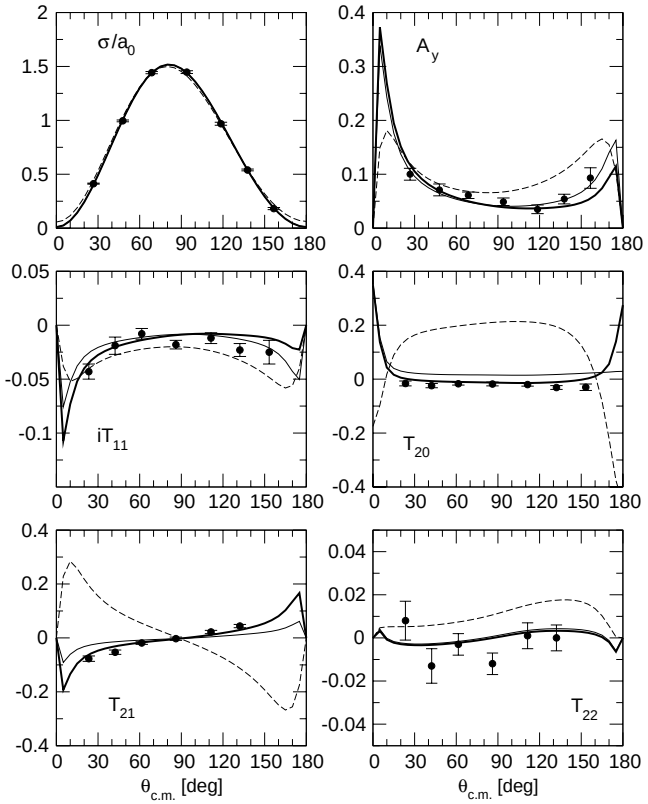

Fig. 2. As in fig. 1 but for $E_{\rm c.m.} = 3.33$ MeV. The experimental values are from ref. [22].

On the contrary, for the observables T_{20} and T_{21}, large discrepancies can be observed. The problems were traced back [20], to an overprediction of the spin-flip electric dipole E_1 reduced matrix elements (RMEs) (namely, those arising from the transitions where the p-d spins in the incident channel are coupled to $S = 3/2$). When the same RMEs were computed in the long-wavelength approximation (LWA) at leading order (thick solid lines in fig. 1) also the observables T_{20} and T_{21} were rather well reproduced.

It was interesting, therefore, to investigate if the same also happens at $E_{\rm c.m.} = 3.33$ MeV. The results for this energy are reported in fig. 2. The notation is similar to that of fig. 1. As can be seen by inspecting fig. 2, there is a good overall agreement with the experimental data, except for the observables T_{20} and T_{21}. Again, in the calculation of the spin-flip E_1 RMEs with the LWA at leading order, the discrepancies between theoretical and experimental results disappear.

Interestingly, an analysis of the next-to-leading-order terms in the LWA performed in ref. [20], has shown that they give a sizable contribution to the spin-flip E_1 RMEs, showing the inadequacy of the use of the leading order only for the calculation of this small spin-flip transition matrix elements. The origin of the discrepancies observed in the T_{20} and T_{21} observables is still unclear.

3 Muon capture

The μ^- weak capture on ^{3}He can occur through three different hadronic channels:

$$\mu^- + {}^3\mathrm{He} \to {}^3\mathrm{H} + \nu_\mu \quad (70\%) \ , \tag{3}$$

$$\mu^- + {}^3\mathrm{He} \to n + d + \nu_\mu \quad (20\%) \ , \tag{4}$$

$$\mu^- + {}^3\mathrm{He} \to n + n + p + \nu_\mu \quad (10\%) \ . \tag{5}$$

The focus of the present section is on the first process. Some of the nuclear-physics issues in muon capture have been reviewed recently in ref. [25]. When the triton polarization is not detected, the differential capture rate for the reaction (3) is given by

$$\frac{\mathrm{d}\Gamma}{\mathrm{d}(\cos\theta)} = \frac{1}{2}\Gamma_0 \Bigg[1 + A_v P_v \cos\theta + A_t P_t \left(\frac{3}{2}\cos^2\theta - \frac{1}{2} \right) + A_\Delta P_\Delta \Bigg] \ , \tag{6}$$

where Γ_0 is the total capture rate, A_v, A_t and A_Δ angular-correlation parameters and θ is the angle between the muon polarization and the ^{3}H recoil. The coefficients P_v, P_t and P_Δ are linear combinations of the probabilities $P(f,\, f_z)$ of finding the ^{3}He μ^- system in the total-spin state $|f\, f_z\rangle$, and are defined as [26,27]

$$\begin{aligned} P_v &= P(1,1) - P(1,-1) \ , \\ P_t &= P(1,1) + P(1,-1) - 2\,P(1,0) \ , \\ P_\Delta &= P(1,1) + P(1,-1) + P(1,0) - 3\,P(0,0) \ . \end{aligned} \tag{7}$$

Therefore, P_v and P_t are proportional to the vector and tensor polarizations of the $f = 1$ state, respectively, while P_Δ indicates the deviation of the $f = 0$ population density from its statistical factor 1/4. Because of the small energy splitting between the $f = 0$ and $f = 1$ hyperfine states (1.5 eV) compared to the μ^- ^{3}He binding energy, and hence small deviation of $P(f,\, f_z)$ from its statistical value, direct measurements of the angular-correlation parameters are rather difficult [25,28,27].

The results reported below have been obtained using either the AV18/UIX interactions or the older Argonne v_{14} (AV14) two-nucleon interaction [29] in conjunction with the the Tucson-Melbourne (TM) three-nucleon interaction [30]. Note that both three-nucleon interactions have been adjusted to reproduce the triton binding energy.

Results for the capture rate Γ_0 and angular-correlation parameters A_v, A_t, and A_Δ are presented in table 1. The uncertainty (in parenthesis) in the predicted values is due to the uncertainty in the determination of the $N\Delta$ transition parameter g_A^*, as discussed in the introduction. The latter reflects the experimental error in the Gamow-Teller matrix element of tritium β-decay.

Inspection of table 1 shows that the theoretical determination of the total capture rate Γ_0, when the AV18/UIX and AV14/TM Hamiltonian models are used, is within 1%

Table 1. Capture rate Γ_0 (s^{-1}) and angular-correlation parameters A_v, A_t, and A_Δ, calculated using PHH wave functions corresponding to the AV18/UIX and AV14/TM Hamiltonian models, are compared with the experimental results. The theoretical uncertainties, shown in parentheses, reflect the uncertainty in the determination of the $N\Delta$ transition axial coupling constant g_A^*. The experimental values of Γ_0 and A_v have been taken from refs. [31] and [28], respectively. Here, we have assumed $R_{PS} = 1$ in eq. (2).

Observable	AV18/UIX	AV14/TM	Expt.
Γ_0	1484(8)	1486(8)	1496(4)
A_v	0.5350(14)	0.5336(14)	0.63(15)
A_t	−0.3650(9)	−0.3659(9)	
A_Δ	−0.1000(16)	−0.1005(17)	

Table 2. Effects of the inclusion of the two-body currents for the muon capture rate Γ_0 (in s^{-1}) and angular-correlation parameters A_v, A_t, and A_Δ. The PHH wave functions are obtained using the AV18/UIX Hamiltonian model. The column labeled "One-body" lists the contributions associated with the one-body vector and axial charge and current operators. The column labeled "Mesonic" lists the results obtained by including, in addition, the contributions from meson-exchange mechanisms. Finally, the column labeled "Δ" lists the results obtained by including also the Δ-excitation contributions. The experimental values of Γ_0 and A_v are taken from refs. [31] and [28], respectively. Here, we have assumed $R_{PS} = 1$ in eq. (2).

Observable	One-body	Mesonic	Δ	Expt.
Γ_0	1316	1384	1484	1496(4)
A_v	0.5749	0.5511	0.5350	0.63(15)
A_t	−0.3565	−0.3679	−0.3650	
A_Δ	−0.0686	−0.0810	−0.1000	

of the recent experimental result [31]. When the theoretical and experimental uncertainties are taken into consideration, the agreement between theory and experiment is excellent. Furthermore, the model dependence in the calculated observables is very weak: the AV18/UIX and AV14/TM results differ by less than 0.5%. The agreement between theory and experiment and the weak model dependence mentioned above reflect, to a large extent, the fact that both the AV18/UIX and AV14/TM Hamiltonian models reproduce i) the experimental binding energies as well as the charge and magnetic radii [32] of the trinucleons; ii) the Gamow-Teller matrix element in tritium β-decay. The value for the angular-correlation parameter A_v listed in table 1 is also in reasonable agreement with the corresponding experimental result which has a rather large error, however.

The contributions of the different components of the weak current and charge operators to the observables are reported for the AV18/UIX model in table 2. The column labeled "One-body "lists the contributions associated with the one-body terms of the vector and axial charge and current operators, including relativistic corrections proportional to $1/m^2$. The column labeled "Mesonic"lists the results obtained by including, in addition, the contributions from two-body vector and axial charge and current operators, associated with pion- and vector-meson-exchanges. Finally, the column labeled "Δ"lists the values of the observables obtained by including the contributions arising from Δ-excitation.

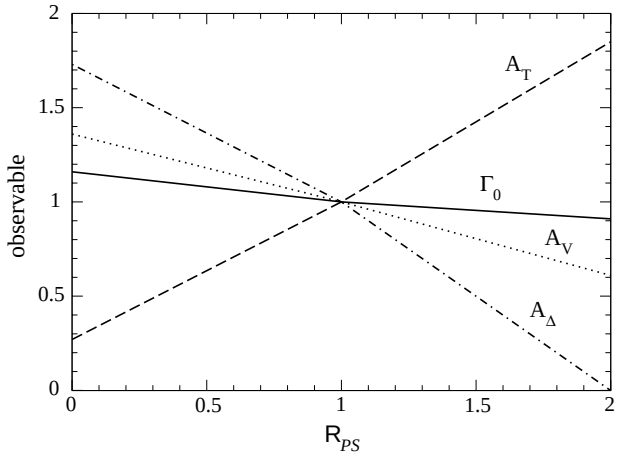

Fig. 3. Variation of the capture rate Γ_0 and angular-correlation parameters A_v, A_t, and A_Δ with the parameter R_{PS} entering the expression for the induced pseudo-scalar coupling G_{PS} given in eq. (2). The AV18/UIX PHH wave functions are used. For each observable, the ratio between the result obtained with the given value of R_{PS} and that one with the PCAC value $R_{PS} = 1$ is plotted as function of R_{PS}.

Among the observables, Γ_0 and A_Δ are the most sensitive to two-body contributions in the weak current. These are in fact crucial for reproducing the experimental capture rate, see table 2.

An important motivation of the present work is to test the sensitivity of the muon capture observables to the induced pseudo-scalar form factor G_{PS} and, eventually, infer its value from the Γ_0 measurement. Therefore, we have repeated the calculation using AV18/UIX PHH wave functions and several different values of the parameter R_{PS}, defined in eq. (2). The variation of each observable in terms of R_{PS} is displayed in fig. 3. The angular-correlation parameters, in particular A_t and A_Δ, are more sensitive to changes in R_{PS} than the total capture rate, as first pointed out in ref. [26]. A precise measurement of these polarization observables could therefore be useful to ascertain the extent to which the induced pseudo-scalar form factors deviate from their PCAC values.

By enforcing the perfect agreement between the experimental and theoretical values, taken with their uncertainties, for the total capture rate Γ_0, it is possible to obtain an estimate for the range of values allowed for R_{PS}, and we have found

$$R_{PS} = 0.94 \pm 0.06 \ . \tag{8}$$

This 6% uncertainty is smaller than that found in previous studies [27,33,34]. This substantial reduction in uncertainty can be traced back to the procedure used to

constrain the (model-dependent) two-body axial currents discussed in the introduction.

4 Summary and outlook

We have reported new calculations of p-d radiative capture observables at energies above the DBT, and of observables in the process $^3\mathrm{He}(\mu^-,\,\nu_\mu)^3\mathrm{H}$. These calculations have been based on the Argonne v_{18} two-nucleon and Urbana IX three-nucleon interactions, and have used accurate bound and continuum wave functions, obtained with the PHH method. The model for the EM- and weak-transition operators has been taken to consist of one- and two-body components. In recent studies, this theory has been shown to correctly predict the static properties of the trinucleons [32], as well as their associated elastic and transition electromagnetic form factors.

A satisfactory description of measured p-d capture observables at $E_{\mathrm{c.m.}} = 3.33$ MeV has emerged with the exception of the T_{20} and T_{21} tensor analyzing powers. Interestingly, the very same discrepancies were observed also below the DBT, namely at $E_{\mathrm{c.m.}} = 2$ MeV. In order to clarify the origin of these discrepancies, we plan to extend the calculation of p-d capture observables at higher energies, and to investigate alternative models for short-range two-body EM currents.

In regard to the muon capture process, we have found that the predicted total rate is in agreement with the experimental value, and has only a weak model dependence: the AV18/UIX and AV14/TM results differ by less than 0.5%. The weak model dependence can be traced back to the fact that both Hamiltonians reproduce the binding energies, charge and magnetic radii of the trinucleons, and the Gamow-Teller matrix element in tritium β-decay.

It is important to note that, if the contributions associated with two-body terms in the axial current were to be neglected, the predicted capture rate would be 1316 (1318) s^{-1} with AV18/UIX (AV14/TM), and so two-body mechanisms are crucial for reproducing the experimental value. The present work demonstrates that the procedure adopted for constraining these two-body contributions leads to a consistent description of available experimental data on weak transitions in the three-body systems. It also corroborates the robustness of our recent predictions for the cross-sections of the proton weak captures on ^{1}H [13] and ^{3}He [15,14], which were obtained with the same model for the nuclear weak current.

Finally, it would be interesting to extend our investigation to the $^3\mathrm{He}(\mu^-,\nu_\mu)nd$ and $^3\mathrm{He}(\mu^-,\nu_\mu)nnp$ processes, both of which have been studied experimentally in ref. [35] and theoretically in ref. [36]. Work along these lines is vigorously being pursued.

The work of R.S. is supported by the U.S. Department of Energy contract number DE-AC05-84ER40150 under which the Southeastern Universities Research Association (SURA) operates the Thomas Jefferson National Accelerator Facility.

References

1. A. Kievsky *et al.*, Phys. Rev. C **58**, 3085 (1998).
2. W. Glöckle, H. Witala, D. Hüber, H. Kamada, J. Golak, Phys. Rep. **274**, 107 (1996).
3. A. Kievsky, S. Rosati, W. Tornow, M. Viviani, Nucl. Phys. A **607**, 402 (1996).
4. R. Schiavilla, V.R. Pandharipande, D.O. Riska, Phys. Rev. C **40**, 2294 (1989).
5. R. Schiavilla, D.O. Riska, Phys. Rev. C **43**, 437 (1991).
6. J. Carlson, R. Schiavilla, Rev. Mod. Phys. **70**, 743 (1998).
7. T.R. Hemmert, B.R. Holstein, N.C. Mukhopadhyay, Phys. Rev. D **51**, 158 (1995).
8. J.D. Walecka, in *Muon Physics; Weak Interactions*, edited by V.W. Hughes, C.S. Wu (Academic Press, New York, 1975) p. 114.
9. J.D. Walecka, *Theoretical Nuclear and Subnuclear Physics* (Oxford University Press, New York, 1995).
10. D.O. Riska, Phys. Scr. **31**, 471 (1985).
11. R. Schiavilla, R.B. Wiringa, V.R. Pandharipande, J. Carlson, Phys. Rev. C **45**, 2628 (1992).
12. M. Kirchbach, D.O. Riska, K. Tsushima, Nucl. Phys. A **542**, 616 (1992).
13. R. Schiavilla *et al.*, Phys. Rev. C **58**, 1263 (1998).
14. L.E. Marcucci *et al.*, Phys. Rev. C **63**, 015801 (2001).
15. L.E. Marcucci, R. Schiavilla, M. Viviani, A. Kievsky, S. Rosati, Phys. Rev. Lett. **84**, 5959 (2000).
16. A. Kievsky, S. Rosati, M. Viviani, Nucl. Phys. A **551**, 241 (1993).
17. A. Kievsky, S. Rosati, M. Viviani, Nucl. Phys. A **577**, 511 (1994).
18. M.K. Smith, L.D. Knutson, Phys. Rev. Lett. **82**, 4591 (1999).
19. M. Viviani, R. Schiavilla, A. Kievsky, Phys. Rev. C **54**, 534 (1996).
20. M. Viviani *et al.*, Phys. Rev. C **61**, 064001 (2000).
21. A. Kievsky, M. Viviani, S. Rosati, Phys. Rev. C **64**, 024002 (2001).
22. F. Goeckner, W.K. Pitts, L.D. Knutson, Phys. Rev. C **45**, R2536 (1992).
23. R.B. Wiringa, V.G.J. Stoks, R. Schiavilla, Phys. Rev. C **51**, 38 (1995).
24. B.S. Pudliner, V.R. Pandharipande, J. Carlson, R.B. Wiringa, Phys. Rev. Lett. **74**, 4396 (1995).
25. D.F. Measday, Phys. Rep. **354**, 243 (2001).
26. W.-Y.P. Hwang, Phys. Rev. C **17**, 1799 (1978).
27. J.G. Congleton, H.W. Fearing, Nucl. Phys. A **552**, 534 (1992).
28. P.A. Souder *et al.*, Nucl. Instrum. Methods Phys. Res. A **402**, 311 (1998).
29. R.B. Wiringa, R.A. Smith, T.A. Ainsworth, Phys. Rev. C **29**, 1207 (1984).
30. S.A. Coon *et al.*, Nucl. Phys. A **317**, 242 (1979).
31. P. Ackerbauer *et al.*, Phys. Lett. B **417**, 224 (1998).
32. L.E. Marcucci, D.O. Riska, R. Schiavilla, Phys. Rev. C **58**, 3069 (1998).
33. J.G. Congleton, E. Truhlìk, Phys. Rev. C **53**, 956 (1995).
34. J. Govaerts, J.-L. Lucio-Martinez, Nucl. Phys. A **678**, 110 (2000).
35. S.E. Kuhn *et al.*, Phys. Rev. C **50**, 1771 (1994).
36. R. Skibinski, J. Golak, H. Witala, W. Glöckle, Phys. Rev. C **59**, 2384 (1999).